FLUID IDENTIFICATION IN HEAVY OIL RESERVOIRS BY NUCLEAR MAGNETIC RESONANCE AT ELEVATED TEMPERATURE

Matthias Appel, J. Justin Freeman, Rod B. Perkins
Shell E&P Technology Company, Bellaire Technology Center, Houston, TX

Terence P. O'Sullivan
Aera Energy LLC, Bakersfield, CA

Abstract

Nuclear Magnetic Resonance (NMR) has developed into a powerful petrophysical tool for reservoir characterization partly because NMR logging tool response can be closely simulated by laboratory NMR measurements at reservoir conditions. Recently developed laboratory capabilities for performing NMR experiments as a function of temperature and pressure enables the forward modeling of the logging tool data and provide insights that are useful in heavy oil reservoirs.

We report results of laboratory NMR experiments on core and bulk oil samples taken from a heavy oil reservoir that is undergoing steam flood. The interpretation of wireline NMR data acquired from this reservoir is challenging because the NMR relaxation time of the high viscosity oil overlaps with that of the capillary bound brine even at water-wet conditions. The standard approach of using the contrast in diffusivity between oil and brine failed due to restricted diffusion. However, by measuring and comparing NMR relaxation data acquired at various temperatures, we were able to distinguish the different pore fluids. As expected, T_2 relaxation times for heavy oil cores at 75F are very fast – less than 10 msec. Consistent with NMR theory, the data indicate that T_2 increases with temperature, but even at temperatures of 210F, the T_2 relaxation time for a native state core with porosity greater than 30% and permeability greater than 1 darcy is almost entirely below 30 ms. These experiments represent a new approach of applying laboratory NMR measurements on core samples to directly support the interpretation of wireline NMR data, especially in heavy oil reservoirs.

Introduction

Nuclear magnetic resonance (NMR) log data were acquired in a San Joaquin Valley (California, USA) heavy oil reservoir that is part of an active steam flood. The data were reviewed with the objective of determining oil, free water and capillary bound water volumes in order to optimize the reservoir development program. Identification of free water is particularly important because disposal of produced water is the major constraint on increased oil production.

Interpretation of conventional log data to determine free water volume in these reservoirs can be difficult because water salinities are low, but perhaps more importantly because grain size analysis data suggest that capillary bound water volume varies significantly. NMR has been successfully used to differentiate bound and free water in light oil reservoirs, but so far NMR has not been extensively used in heavy oil reservoirs. The limited application of NMR to heavy oil reservoirs is at least partly due to the fact that light oil NMR models don't work in heavy oil. To build NMR models, NMR data are required from bulk oil and core samples.

NMR bulk oil data that could be used to guide the log interpretation for heavy oil reservoirs are limited, but some data are available. Morriss et al. (1994) measured T_2 relaxation spectra for (77^oF) bulk oil samples with viscosities between 2.7 and 4304 cp and found that heavy oils have broad T_2 relaxation spectra with mean T_2 relaxation times that are very fast - less than 10 msec, as compared to more than 200 msec for light oils. Morriss et al. also demonstrated that a relationship exists between the mean T_2 for bulk oil samples and the oil viscosity; however, this relationship is not applicable to oils with viscosities greater than 1000 cp. Viscometer measurements over a range of temperatures (Figure 1) shows that oil viscosity in

the target reservoir can be as high as 20,000 cp - at this viscosity there are no available data on bulk oil NMR response.

With regard to NMR core measurements, the target reservoir is very similar to other heavy oil reservoirs in the San Joaquin Valley: porosities are greater than 30%, air permeabilities are greater than 1 darcy, and oil gravity is less than 14 API. Billions of barrels of heavy oil exist in similar reservoirs in this basin, with most of the oil produced by steam flood. Reservoir temperatures in active steam floods vary from over 300 ^{o}F in the steam chest, to less than 100 ^{o}F in intervals that have not been steamed. NMR data for cores from these reservoirs are rare or non-existent, and NMR core data are certainly unavailable over the range of temperatures that exist in active steam floods.

If the reservoir were to contain light oil, standard NMR theory predicts that T_2 relaxation rates for native state core samples would be dominated by surface relaxation and relaxation due to diffusion, with only negligible contributions from bulk relaxation. By calibration with core, interpretation methods that rely on differences in the relaxation times (T_1 and T_2) and diffusivity of capillary bound water, oil and free water could successfully be used to identify these components. With heavy oil, however, the short relaxation time causes the oil peak to interfere with capillary bound water peak even at water-wet conditions. In addition, the evaluation of the measured data cannot be based on diffusion contrast between oil and brine since diffusion does not significantly contribute to the relaxation of the pore fluids. Moreover, diffusion of capillary bound brine is restricted, and therefore, the measured apparent diffusivity of the capillary bound brine and the diffusivity of the heavy oil are very similar. Finally, because of the short T_2 relaxation times of both the capillary bound brine and the heavy oil, NMR techniques with applied magnetic field gradients (like Pulsed Field Gradient NMR or T_2 relaxation measurements with applied constant magnetic field gradients) are not practical.

From this discussion, it is apparent that in order to develop a strategy for evaluating heavy oil NMR log data, additional measurements are needed both on the bulk oil and native state reservoir responses. It is also clear that these measurements are needed over a range of temperatures similar to those in the reservoir.

Experimental

Core measurements were made on a single plug taken from preserved conventional core. Routine analysis of adjacent plugs indicates that porosity is approximately 35%, oil saturation is 75% and water saturation is 25%. The sample is described as a dark brown, very-fine to medium-grained, slightly silty and micaceous sand with dark stain and dull gold fluorescence. The sand is poorly consolidated and a water-wet saturation state is indicated from core analysis of adjacent plugs and well-log data. For the NMR investigations, the core material was compacted at 1000 psi hydrostatic pressure to obtain a pore structure that represents in-situ formation conditions. Bulk oil measurements were made on a produced oil sample.

The NMR response was measured using a commercial low-field benchtop NMR analyzer working at 2 MHz proton resonance frequency. The core plug was wrapped with NMR-silent material to avoid any loss of saturation during the experiments. The wrapped plug was contained in an NMR-silent core holder capable of sustaining hydrostatic overburden pressure of 1000 ± 150 psi during the measurements. Measurements were made at temperatures that varied between 75F and 210F with an accuracy of ± 5F. The NMR response of the bulk oil sample was measured using a custom-built, NMR-silent pressure cell at conditions similar to those used for the core sample.

The transverse relaxation time spectra, T_2, of the pore fluids was determined using a Carr-Purcell-Meiboom-Gill (CPMG) pulse sequence with inter-echo spacings of 200 μs, 600 μs and 1.2 msec. The experiments discussed in this paper were performed without external magnetic field gradients. For each sample, the delay time between subsequent pulse sequences was chosen to be at least five times longer than the longest component of its longitudinal (T_1) relaxation time spectrum to guarantee a complete polarization for each experiment. A sufficient number of spin echoes were acquired to assure a complete attenuation of the CPMG decay to noise level. Depending on the experimental parameters, a few hundred to several thousand echo trains were stacked to obtain a constant signal-to-noise ratio of 50 for all experiments. CPMG signal decay curves were then inverted to distributions of relaxation times using a distributed exponential fitting procedure with an optimization of the regularization parameter according to the signal-to-noise of the experiment.

Results

Shift of Transverse Relaxation Rate of Pore Fluids. Figure 2 shows the spectra of the transverse relaxation time, T_2, for the core sample 2241A measured at various temperatures using the 200 μs inter-echo spacing. In this figure, the measured T_2 spectra are illustrated by symbols; the solid lines are the results of calculations made to separate overlapping relaxation peaks which will be discussed later. For these measurements, the temperature was first increased from 75F to 210F and then reduced to 75F. Two main features can be noted from the measured data. First, the T_2 relaxation spectrum is clearly shifted to longer relaxation times with increasing temperature. Second, the shape of the T_2 spectra significantly changes with temperature.

Core relaxation spectrum 1, measured at a temperature of 75F, contains three distinct peaks. With increasing temperature, these three peaks are shifted towards longer relaxation times at different rates This causes the peaks to overlap so that at the highest measured temperature (210F, spectrum 3), there is a single T_2 peak. Even at 210F, however, there is very little T_2 signal beyond 30 msec.

Comparison of core spectra 1 and 7, both measured at 75F, shows that the heating and cooling cycle has changed the NMR signature of the sample. In spectra 7, the two left peaks of spectrum 1 have merged to form a single peak, and the far right peak has shifted to a shorter relaxation time. The shift of the far right peak could be attributed to compaction of the unconsolidated core material as a result of heating to 210F with an overburden pressure of 1000 psi. Reduced pore size would increase the contribution of the pore surfaces to the overall relaxation spectrum, shifting the far right T_2-peak to a shorter relaxation time as the ratio of bulk to surface relaxivity decreases. The coalescence of the two left peaks may be related to changes in the molecular structure of the heavy oil as a result of heating. Other explanations for these effects, including changes in wettability or capillary bound water saturation are clearly possible.

In any case, it appears that the spectra 1 – spectra 7 shift is not an experimental artifact. For all T_2 distributions, the area under each relaxation peak is directly proportional to the number of magnetic moments, and therefore the number of protons, in a given T_2 interval. Evaluation of the areas for spectra 1 and 7 in Figure 2 shows that the number of protons that contribute to the two left peaks of spectrum 1 is equal to the number of protons that correspond to the major peak of spectrum 7, confirming that the two left peaks of spectrum 1 have merged to become the major peak of spectrum 7.

Shift of Transverse Relaxation Rate of the Bulk Heavy Oil. In order to unambiguously identify the pore fluids with the measured relaxation peaks, the NMR response of the bulk oil of this formation was measured. Figure 3 shows the T_2-relaxation spectra of the bulk heavy oil measured at four temperatures between 75F and 210F. As in Figure 2, the measured data are illustrated by circles, whereas the solid lines represent the results of calculations made to separate overlapping relaxation peaks. Once again, increasing the temperature from 75F to 210F significantly shifts the T_2-peaks towards longer relaxation times. Additionally, the "single" peak measured at 75F splits into two distinct peaks at higher temperatures with a decreasing intensity of the peak at shorter relaxation times relative to that at longer T_2's. After scaling the measured data to the same number of stacked echo trains, the area underneath all four spectra is the same, showing that the same number of magnetic moments, and, hence, molecules, contributed to the acquired spin echoes.

Discussion

1. Fluid Identification. The overall rate of transverse magnetic relaxation, T_2, of the pore fluid in a porous system is the sum of the bulk, surface, and diffusion relaxation rates,

$$T_2^{-1} = T_{2_{bulk}}^{-1} + r\frac{S}{V} + \frac{1}{12}g^2\gamma^2 TE^2 D \qquad \textbf{(1)}$$

For the surface term, r denotes the surface relaxivity and S/V the surface-to volume ratio of the pore structure. In the diffusion term, D is the diffusion constant of the molecules in resonance, γ the gyromagnetic ratio, g the intensity of the externally applied magnetic field gradients and TE the inter-echo

spacing of the CPMG pulse sequence. This inter-echo spacing, as well as the applied magnetic field gradient are experimentally adjusted parameters (Kenyon, 1997).

All measurements were made in a homogenous background magnetic field without applied magnetic field gradients. CPMG pulse sequences measured at different inter-echo spacings were very similar, indicating that there are no internal magnetic field gradients caused by susceptibility contrasts between the pore fluids and the grain material in the sample. Therefore, the intensity, *g*, of the magnetic magnetic field gradients in Equation 1 is zero, and the T_2 relaxation spectra of the pore fluid in our measurements are determined by bulk and surface relaxation only.

It is commonly assumed that bulk relaxation does not significantly contribute to the overall relaxation rate and that the surface relaxation effects dominate the T_2 spectra. This assumption has mainly been derived from the observation that temperature had no effect on the measured relaxation spectra of about a dozen water-saturated sandstones and carbonates (Latour et al., 1992). In contrast to these experiments, our data show a strong relationship between the temperature and the shape of the T_2 spectra for heavy oil. This change occurs for both the bulk oil phase and for oil as a pore fluid, indicating that bulk relaxation is important for heavy oils. This result is not unexpected, given that the viscosity of the measured oil is on the order of 100,000 cp at room temperature.

Comparing the T2-temperature spectra for the core plug (Figure 2) it is obvious that the individual peaks measured at 75F have merged into a single composite peak at higher temperatures. In order to examine the shift of the individual peaks and to compare their temperature dependence with that of the bulk oil sample, a method was needed to separate the overlapping peaks. The selected method was based on the assumption that the relaxation spectra at 75F identifies three fundamental T_2 peaks, and that spectra 2 through 6 of Figure 2 represent a temperature dependent superposition of these three T_2 peaks at different positions and intensities. Comparison of the 75F and 140F spectra in Figure 2 supports this approach, since it indicates that at 140F spectrum 2 still contains three peaks, but the two left peaks have merged into a peak and a shoulder.

In order to decompose the T_2 spectra, two additional requirements were satisfied. These are that the CPMG decay curves have been acquired with the same signal-to-noise ratio, so that the resolution of the inversion routine will be the same for all measured spectra, and in addition, that no pore fluid has left the pore space during the measurements. This was confirmed gravimetrically and by the constant cumulative NMR signals.

To calculate the position, $x_{0,i}$, and intensity, a_i , of each peak, we assumed that each composite relaxation peak can be described by a log-normal distribution of T_2 relaxation times, and then optimized the relationship:

$$I = \sum_{i=1}^{3} a_i \exp\left\{-\frac{1}{2}\left(\ln\left(\frac{T_2}{x_{0,i}}\right)\Big/ b_i\right)^2\right\} \qquad \textbf{(2)}$$

In Equation 2, b_i determines the width of each log-normal peak. It is obvious that this procedure is not robust since multiple configurations might fit the measured data equally well. However, given the input parameters of core spectrum 1 and crosschecking the calculated positions and intensities for physical relevance, such obtained separation of the overlapping relaxation peaks seems to be reasonable. The solid lines in Figure 2 illustrate the results of the inversion calculations. The sum of intensities of all three individual peaks at a given T_2 value is also calculated and represented by a solid line, which is almost completely covered by the symbols as this separation procedure describes the measured data very well.

A similar procedure was applied to decompose the composite bulk oil peak. For these calculations we assumed a superposition of two log-normal distributions of relaxation times as indicated by the data acquired at 210F and 180F. The results of the calculations are illustrated by solid lines in Figure 3, with the measured data points represented by symbols. The sum of all three individual peaks at a given T_2 is again almost perfectly covered by the data; some minor deviation can only be recognized at the highest T_2-values.

Figure 4 shows the positions of each calculated relaxation peak as function of temperature. In the left diagram, Figure 4a, the peak positions determined by the superposition of the three log-normal peaks are

plotted versus the measured temperatures. The values derived from spectra 1 and 2 of Figure 2 are omitted in this calculation because as discussed above, additional compaction at the highest temperature might have changed the pore structure. In order to illustrate the temperature procedure of the experiment, the temperatures are plotted with the highest values first. Obviously, each peak follows its own temperature behavior, with the far right peaks in Figure 2 showing the strongest dependence on temperature (squares), whereas the position of the peaks at the shortest relaxation times of the core sample T_2 spectra is changed by about a factor of two only (triangles).

In the right diagram, Figure 4b, the temperature behavior of each calculated relaxation peak is illustrated in an Arrhenius plot. If the temperature variation of T_2 is governed by single activation energy, E_A, an Arrhenius diagram of the measured peak shifts yields a straight line with the slope proportional to the activation energy. Our measured data follow this prediction very closely, with activation energies between 9!2 kJ/mol for the left relaxation peak, 19!3 kJ/mol for the middle peak and 29!3 kJ/mol for the right T_2 peak shown in Figure 2.

The observed peak shifts measured for the bulk oil sample are shown in Figure 5. Similar to Figure 4, Figure 5a represents the peak positions derived from the superposition of two log-normal peaks as function of temperature. Figure 5b displays the peak shift in an Arrhenius plot. As for the pore fluids in Figure 4, the two relaxation peaks of the bulk oil differ significantly in their temperature behavior. The variation of the relaxation time with temperature is determined by an activation energy of 17!2 kJ/mol for the left relaxation peak shown in Figure 3 and a value of 38!3 kJ/mol for the right T_2 peak.

The calculated activation energies can be used to tie the measured T_2 relaxation peaks to pore fluids based on the fact that a temperature variation should have a stronger impact on the bulk fluid than on the fluids in pore space. As a result, the activation energies for the bulk oil phase should be higher than those determined for the same oil in the core sample. From this argument, the two far left peaks (peaks 1 and 2, illustrated by triangles and circles, respectively, in Figure 4) of the relaxation spectra shown in Figure 2 correspond to the oil phase because the temperature dependencies of these peaks are characterized by activation energies that are smaller than the activation energies measured for the bulk oil. In contrast to this, the activation energy of the far right peak of Figure 2 (illustrated by squares in Figure 4) is larger than the activation energy of the left oil peak and, within the error bars, comparable to the one of the right peak of the bulk oil. It is assumed that this part of the T_2 spectrum of the pore fluids corresponds to capillary bound brine.

The identification of the measured relaxation peaks with pore fluid can also be based on a discussion of the relaxation rates of each peak. Equation 1 shows that interaction of the magnetic moments with surrounding grain surfaces increases the overall relaxation rate according to the surface relaxivity, r, and the surface-to-volume ratio, S/V, of the pore structure. As a result, the relaxation times, i.e., the inverse relaxation rates, of fluids in pore space will always be shorter than the corresponding values of the bulk fluid phases. Comparing Figure 4a with Figure 5a, it is obvious that for all measured temperatures, the T_2 times of the far right core peak in Figure 2 (illustrated by squares in Figure 4) is comparable to or even longer than any of the relaxation times of the bulk oil. It can, therefore, be deduced that the far right peak of the NMR response of the pore fluid is not caused by the oil phase.

Finally, in this discussion of pore fluid identification, it needs to be noted that reconciliation of the interpretation presented here with the routine core analysis data is incomplete. While the core analysis reports a water saturation of 25%, the T_2 area representing the capillary bound water in this core is estimated to be less than 10% of pore volume. The exact cause of this discrepancy is presently unclear. One possibility is that the mica in this core contains significant amounts of water which appear at very short T_2 times. Additional testing, using Soltrol or other water-soluble chemicals to eliminate the water signal is planned.

2. Viscosity Estimation. For bulk fluids, the NMR relaxation time at a given temperature is directly related to the fluid viscosity (Abragam, 1961, Brown, 1961). When the relaxation process is dominated by dipolar coupling and the correlation time for molecular motion is much less than the inverse Larmor frequency of the precessing magnetic moments, the relaxation rate of protons is given by

$$\frac{1}{T_2} = \frac{1}{T_1} = \frac{2\pi g^4 \hbar^2 a^3}{k_B b^6}\left(1 + \frac{3\pi N b^6}{5a^3}\right)\frac{\eta}{T} \qquad \textbf{(3)}$$

In Equation 3, η denotes the fluid viscosity, T the temperature, N the density of magnetic moments, g the gyromagnetic ratio, $\hbar$ is the Planck's constant divided by 2π and k_B Boltzmann's constant. The constant a is the radius of the hard sphere to which the molecule is approximated by Stokes formula and b is the internuclear distance between protons of the same molecule. The first term in Equation 3 is due to intramolecular relaxation from rotational diffusion, whereas the second term describes intermolecular relaxation from translational diffusion. For both the translational and the rotational diffusion, the molecule is assumed to obey Stokes' law.

For hydrocarbons in a limited viscosity range, Vinegar et al. have derived correlations to estimate viscosity-temperature relations (Vinegar, 1995). For light hydrocarbons, they found

$$T_2 \cong T_1 = \frac{1.2T}{298\eta} \qquad \textbf{(4)}$$

In Equation 4, the relaxation times, T_2 and T_1, are in seconds, T is the absolute temperature in Kelvin, and η the viscosity in cp. Morris et al. used an expression similar to Equation 4 to estimate oil viscosities from NMR logging in the Belridge Diatomite (Morris et al., 1994). However, neither for heavy oils nor for live oils any expression exists to date to relate the magnetic relaxation times to the fluid viscosity index.

Viscosity was interpolated from the temperature-viscosity relationship shown in Figure 1, for the bulk oil temperatures at which T_2 was measured. These estimated viscosities were plotted against the equation 4 calculated viscosities for the short T_2 (Figure 5, triangle) and long T_2 (Figure 5, circle) bulk oil peaks, as shown in Figure 6. Two features can be noted from this plot. First, for bulk oil viscosities up to about 500 cp (corresponding to temperatures of 210F and 180F, respectively), the viscosities calculated from the T_2 relaxation peaks of the bulk heavy oil either overestimate (using the data of the short T_2 peak) or underestimate (using the data of the long T_2 peak) the measured viscosities. Second, for viscosities higher than about 500 cp (corresponding to oil temperatures of 140F and 75F, respectively), the viscosities calculated from both peaks are systematically smaller than the measured values.

Since the area underneath a relaxation peak represents the number of magnetic moments relaxing with the spectrum of T_2 time constants, a weighted average of both calculated viscosities can be derived using the area ratio of both relaxation peaks in Figure 3. This weighted viscosity average is plotted with diamonds in Figure 6. For the viscosities at 210F and 180F, the weighted average of the NMR-derived viscosities is very close to the values measured for the bulk oil. At 140F and 75F, however, the viscosities derived from both individual relaxation peaks are smaller than the viscometer data, and the weighted average of the NMR-derived viscosities also clearly underestimates the measured values.

The two distinct relaxation peaks measured for the bulk oil and the oil as pore fluid represent two main components of the heavy oil that differ in their viscosities and in the activation energies that govern the viscosity indices of these components. Calculating the weighted average of viscosities from both components using the area underneath each relaxation peak represents the composition of the oil with regard to the two components that can be separated by NMR. For that reason, this weighted average will coincide with the viscometer data as long as the correlation for deriving viscosities from relaxation times is valid for each individual component. In our case, Equation 4 obviously holds for viscosities smaller than about 500 cp. For heavier oils, the viscosity data derived from this correlation are systematically too small.

Since no correlation currently exists to calculate the exact viscosities over the entire temperature range, the absolute viscosity values cannot be derived directly from the NMR data. However, as the ratio

of the area underneath each relaxation peak of the bulk oil represents the composition of the heavy oil of fractions with different viscosities, this peak area ratio by itself correlates very well with the viscometer data. Figure 7 illustrates this correlation. In this diagram, the Figure 1 derived viscosities of the bulk oil at various temperatures are plotted versus the ratio of the areas under each of the two relaxation peaks in Figure 3. For the investigated temperature range, the measured bulk oil viscosity closely follows an exponential relation with the ratio of areas underneath the two T_2 relaxation peaks. After calibration to laboratory data, such a correlation might be used for estimating hydrocarbon properties in viscosity ranges where currently no other relation is available.

Conclusions

We have reported results of laboratory NMR experiments on an unconsolidated core and oil sample from a heavy oil reservoir. By measuring and comparing the spectra of transverse NMR relaxation times on core at various temperatures with the NMR properties of bulk oil, we were able to distinguish the different pore fluids and to identify the response of the oil phase in the NMR signal.

The relaxation spectra of both the bulk heavy oil and the core sample were characterized by overlapping peaks. The individual T_2 peaks could be separated with a model that assumes (i) the T_2 peaks to follow a log-normal distribution, and (ii) that the number of relaxation peaks is the same for all measured temperatures. Comparing the peak positions of the core sample with the NMR response of the bulk oil, the oil signal in the T_2 spectrum of the core sample could be identified. Additionally, from the shift of the relaxation peaks with temperature, an activation energy was determined that further aided in the identification of the measured relaxation peaks with the pore fluids.

Whereas the standard relations for estimating viscosity from NMR relaxation data failed to describe the bulk oil correctly over the entire temperature range, a good correlation was found between the measured viscosities and the ratio of the areas underneath each of the relaxation peaks of the bulk oil. This area ratio represents the composition of the oil with regard to the components that can be distinguished by NMR relaxometry.

These experiments represent a new approach of applying laboratory NMR measurements on core samples to directly support the interpretation of wireline NMR data in heavy oil reservoirs. Additional laboratory data are required to verify and extend the results described here. For the evaluation of NMR log data, the T_2 spectra for the core indicates that even at 210F, there is very little oil signal beyond 30 ms. This suggests that, for similar reservoirs, all NMR T_2 signal beyond 40ms is due to free water. To explore this possibility further, measurement of T_2 spectra for water saturated cores over a range of temperatures, and additional measurements on the cores examined here, using Soltrol to eliminate the water signal, are recommended.

Acknowledgements

The authors wish to thank R.M. Ostermeier, Shell E&P Technology Company, for stimulating discussions. Bonnie Bloeser and Ron Palmer, Aera Energy LLC, also supported this project and provided very useful guidance.

Reference:

Abragam, A., *The Principle of Nuclear Magnetism*, Oxford University Press, Oxford, 1961, Chapter 8.

Fukushima, E., Roeder, S.B.W., *Experimental Pulse NMR – A Nuts and Bolts Approach,* Addison-Wesley Publishing Company, Inc., Reading, Massachusetts, 1981.

Vinegar, H. "NMR Fluid Properties", Proceedings of NMR Short Course, SPWLA 36th Annual Symposium, Paris, France, June 26th , 1995.

Kenyon, W.E., "Petrophysical Principles and Applications of NMR Logging", *The Log Analyst*, 1997, **38**, No. 2, pp. 21-43.

Brown, R.J.S., "Proton Relaxation in Crude Oils", *Nature*, 1961, pp. 387-388.

Morris, C.E., Freedman, R., Straley, C., Johnston, M., Vinegar, H.J., Tutunijan, P.N., "Hydrocarbon Saturation and Viscosity Estimation from NMR Logging in the Belridge Diatomite", SPWLA 35th Annual Logging Symposium, June 19th-22nd, 1994, paper C.

Latour, L.L., Kleinberg, R.L., Sezginer, A., *J. Colloid Interface Sci.*, 1992, **150**, p. 535.

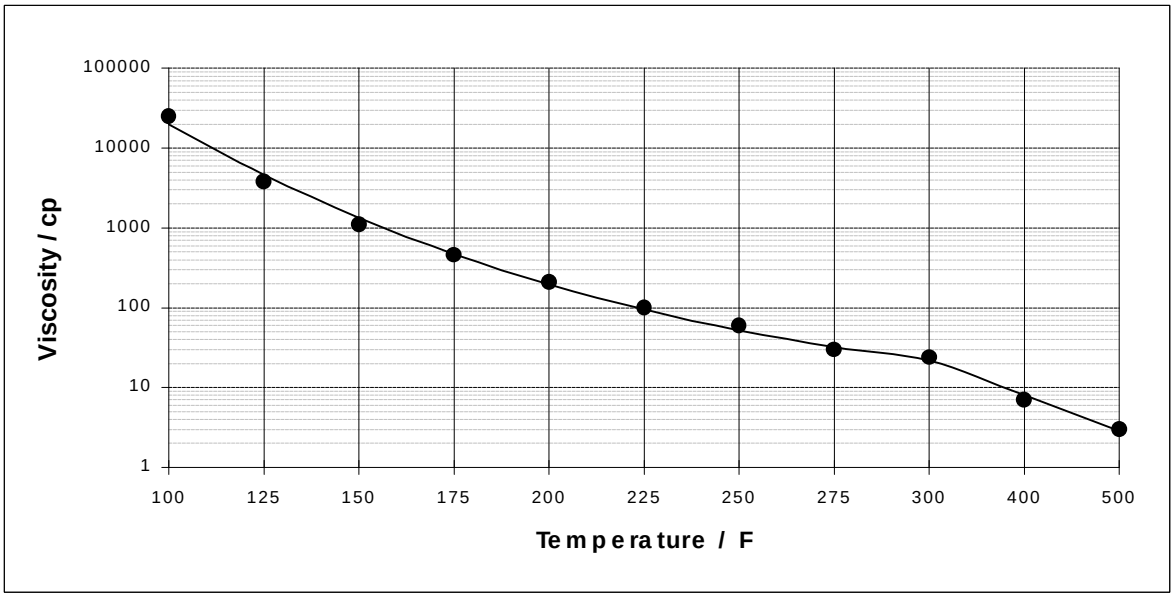

Figure 1: Viscometer-derived temperature-viscosity data for heavy oil produced from the same reservoir as the bulk oil sample used for the NMR study.

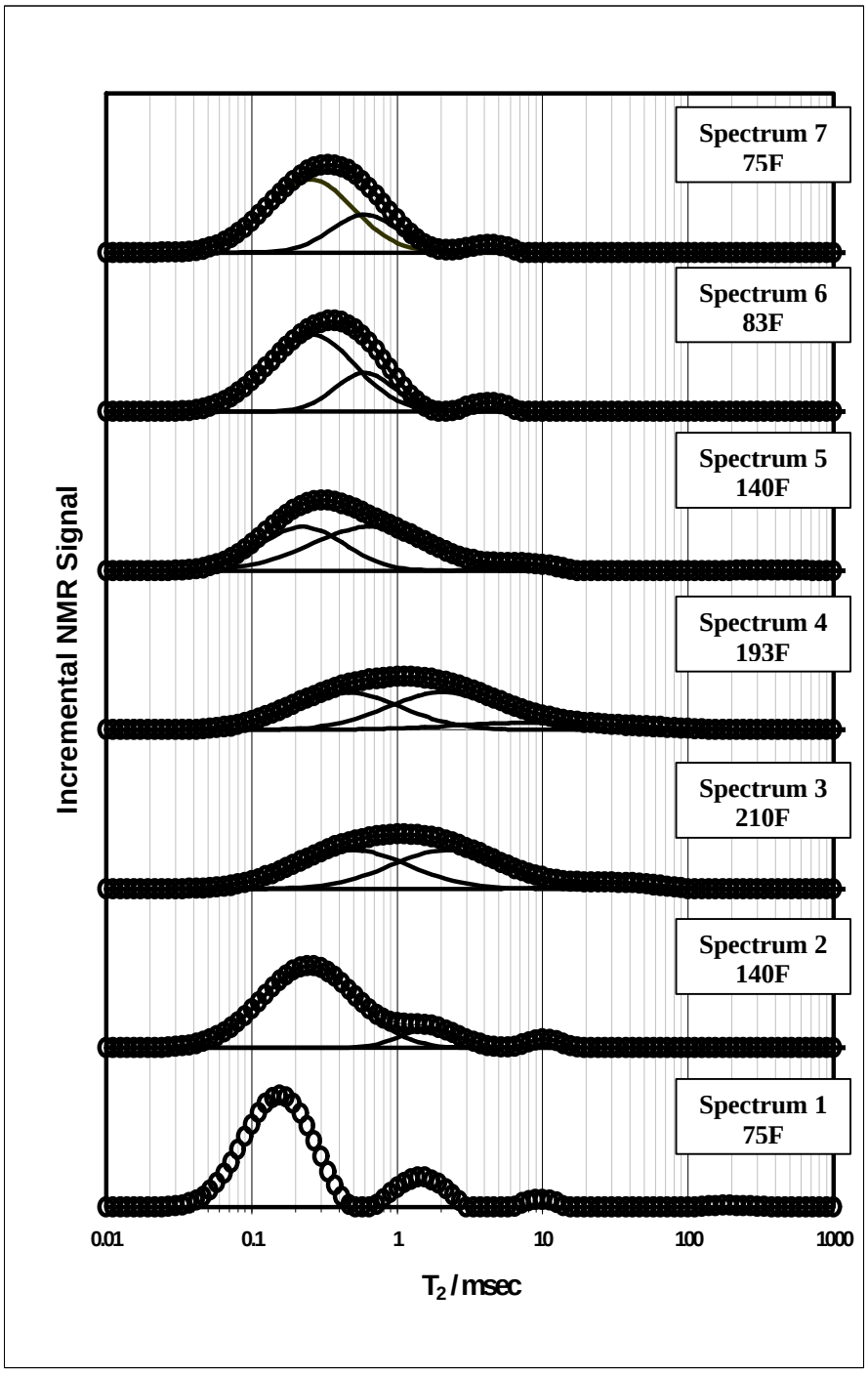

Figure 2: Spectra of the transverse relaxation time, T_2, for the oil- and brine saturated core sample. The temperature was increased from 75F (spectrum 1) to 210F (spectrum 3) and then gradually decreased to 75F. The measured T_2 spectra are illustrated by circles. The solid lines represent the results of calculations made to separate overlapping relaxation peaks.

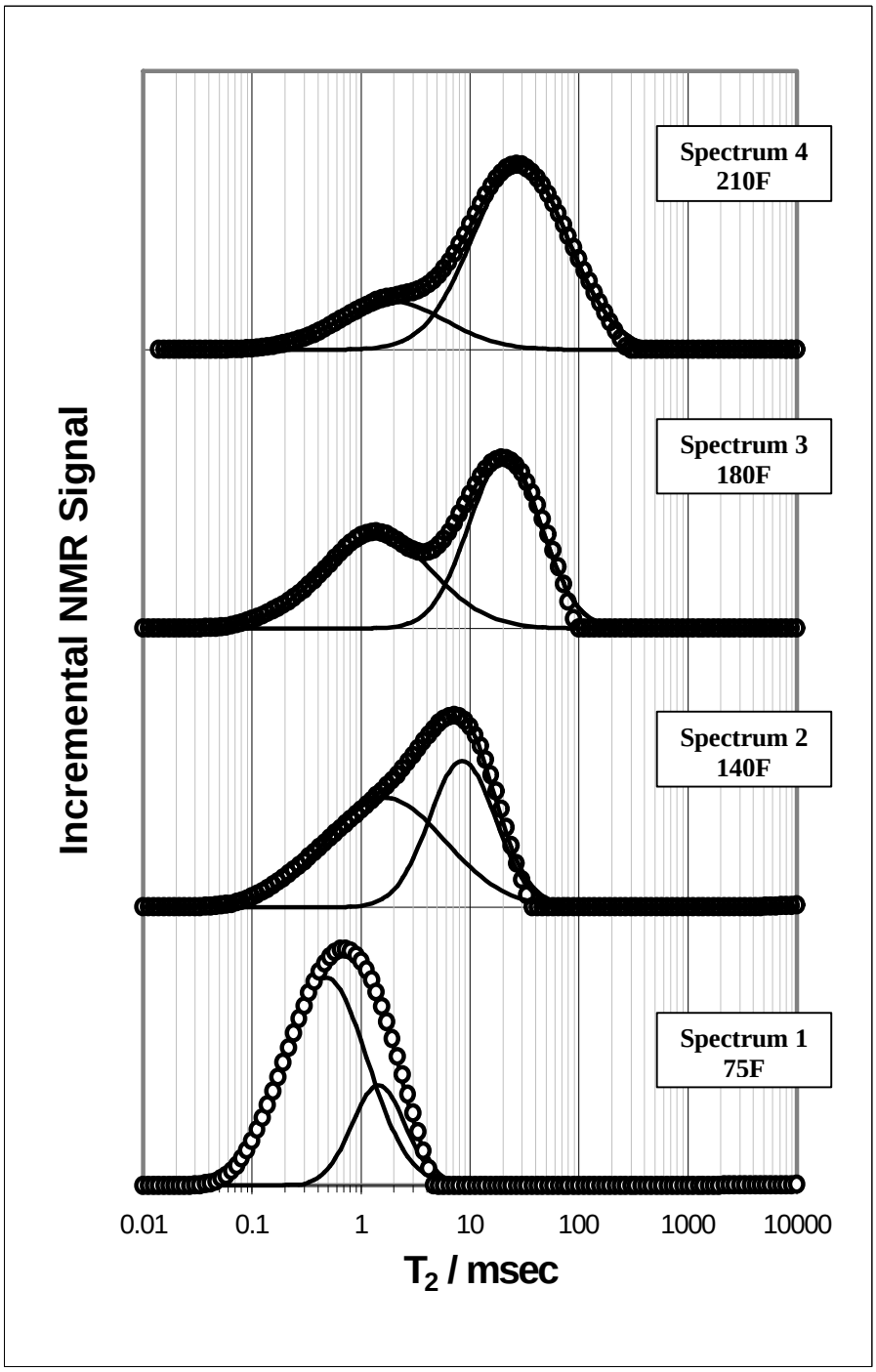

Figure 3: Spectra of the transverse relaxation time, T_2, for the bulk heavy oil sample. The temperature was increased from 75F (spectrum 1) to 210F (spectrum 4). The measured T_2 spectra are illustrated by circles. Note the development of a bimodal relaxation spectrum at higher temperatures. The solid lines represent the results of calculations made to separate overlapping relaxation peaks.

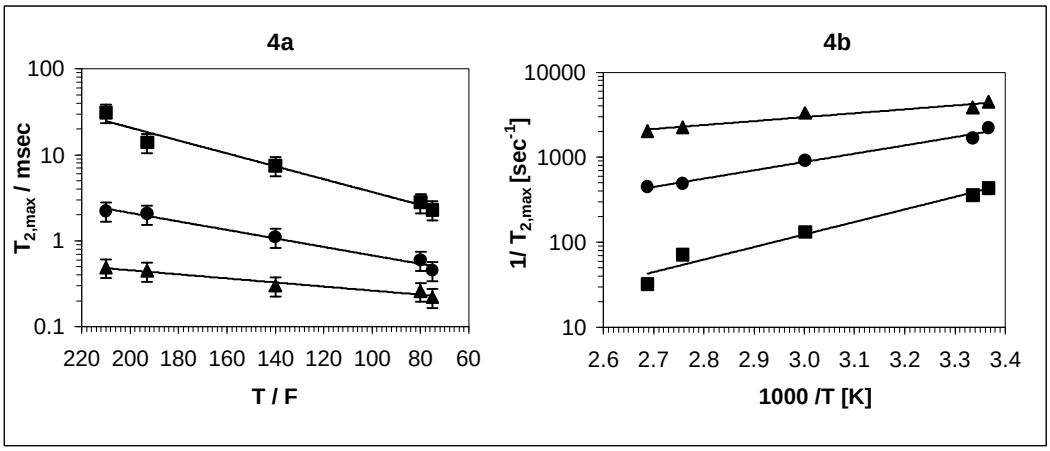

Figure 4: Calculated positions of the T_2 peaks of the core sample. The T_2 spectra of the core sample were characterized by a superposition of three relaxation peaks. **Figure 4a:** Positions of the individual relaxation peaks as a function of temperature. Note the different temperature behaviors for the shortest relaxation peaks (triangles) and the longest relaxation peak (squares). **Figure 4b:** Temperature shift of relaxation rates of core sample plotted in an Arrhenius diagram. The slope of the lines is proportional to the activation energy of the T_2 relaxation process.

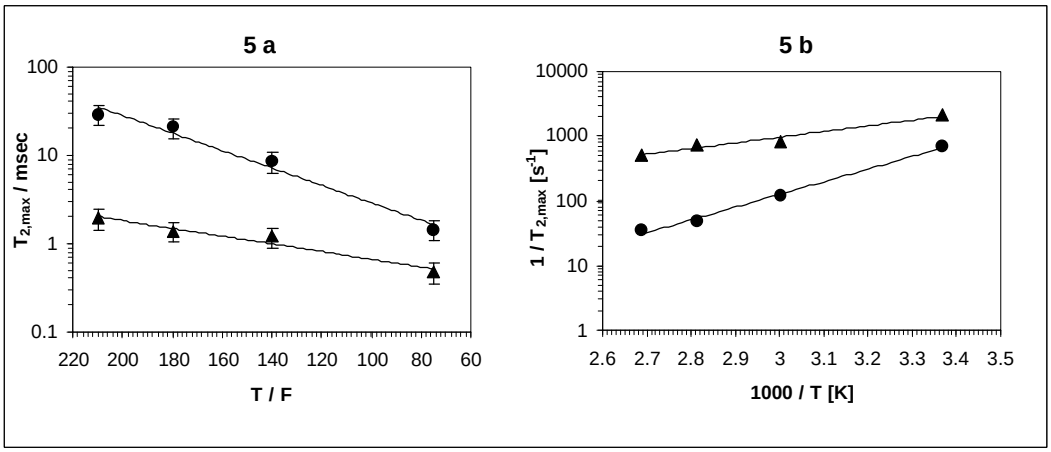

Figure 5: Calculated positions of the T_2 peaks of the bulk oil sample. The T_2 spectra of the oil sample were characterized by a superposition of two relaxation peaks. **Figure 5a:** Positions of the individual relaxation peaks as a function of temperature. Note that the peak at longer relaxation times (circles) shows a stronger dependence on temperature than the peak at shorter T_2's (triangles). **Figure 5b:** Temperature shift of relaxation rates of bulk oil peaks plotted in an Arrhenius diagram. The slope of the lines is proportional to the activation energy of the T_2 relaxation process.

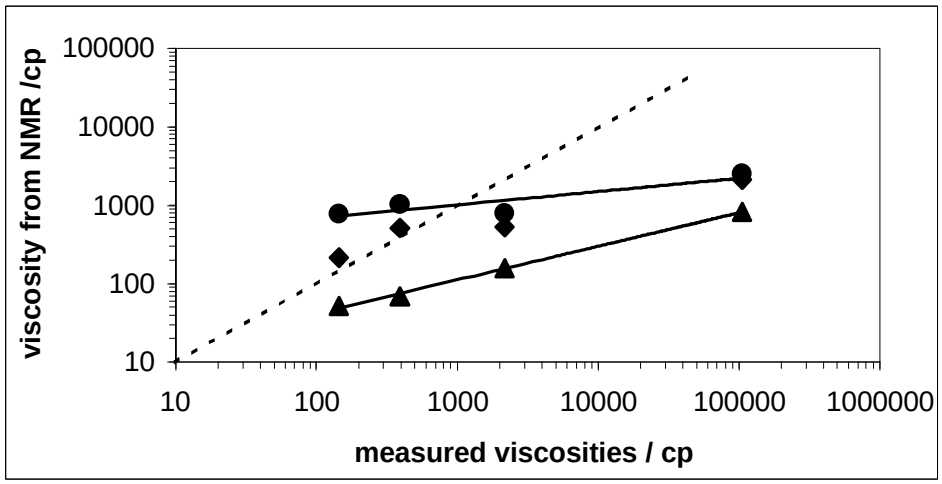

Figure 6: Crossplot of the measured viscosities and viscosities derived from NMR relaxation data using Equation 4. The triangles represent the viscosities derived from the peaks at longer relaxation times, the circles represent viscosities derived from the peaks at shorter T2's. Using the ratio of areas underneath each of the two relaxation peaks at a given temperature, the weighted average of both viscosities was calculated (diamonds). Note the good correlation of the weighted average up to about 500cp measured bulk viscosity. For higher viscosities, Equation 4 is not valid and the NMR data underestimate the fluid viscosity.

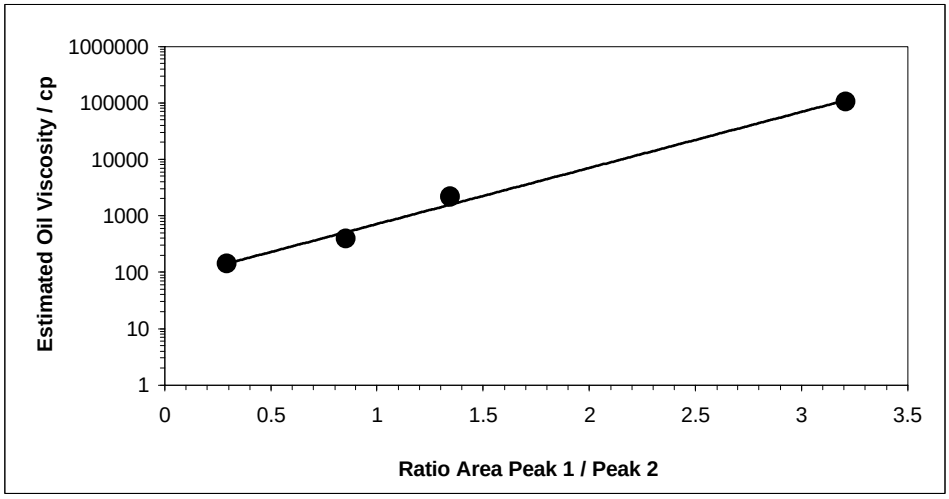

Figure 7: Crossplot of the measured viscosities and the ratio of areas underneath each of the two relaxation peaks at a given temperature for the bulk oil sample. This area ratio represents the composition of the heavy oil with regard to the components that can be distinguished by NMR relaxometry.